CHALMERS
FINITE ELEMENT CENTER

PREPRINT 2005–09

A quasi-planar incident wave excitation for time-domain scattering analysis of periodic structures

David Ericsson, Tomas Halleröd, Börje Emilsson, Anders Bondeson and Thomas Rylander

Chalmers Finite Element Center
CHALMERS UNIVERSITY OF TECHNOLOGY
Göteborg Sweden 2005

CHALMERS FINITE ELEMENT CENTER

Preprint 2005–09

A quasi-planar incident wave excitation for time-domain scattering analysis of periodic structures

David Ericsson, Tomas Halleröd, Börje Emilsson, Anders Bondeson and Thomas Rylander

CHALMERS

Chalmers Finite Element Center
Chalmers University of Technology
SE–412 96 Göteborg Sweden
Göteborg, December 2005

A quasi-planar incident wave excitation for time-domain scattering analysis of periodic structures
David Ericsson, Tomas Halleröd, Börje Emilsson, Anders Bondeson and Thomas Rylander
NO 2005–09
ISSN 1404–4382

Chalmers Finite Element Center
Chalmers University of Technology
SE–412 96 Göteborg
Sweden
Telephone: +46 (0)31 772 1000
Fax: +46 (0)31 772 3595
www.phi.chalmers.se

Printed in Sweden
Chalmers University of Technology
Göteborg, Sweden 2005

Abstract

We present a quasi-planar incident wave excitation for time-domain scattering analysis of periodic structures. It uses a particular superposition of plane waves that yields an incident wave with the same periodicity as the periodic structure itself. The duration of the incident wave is controlled by means of its frequency spectrum or, equivalently, the angular spread in its constituting plane waves. Accuracy and convergence properties of the method are demonstrated by scattering computations for a planar dielectric half-space. Equipped with the proposed source, a time-domain solver based on linear elements yields an error of roughly 1% for a resolution of 20 points per wavelength and second order convergence is achieved for smooth scatterers. Computations of the scattering characteristics for a sinusoidal surface and a random rough surface show similar performance.

1 Introduction

Periodic structures are important in many electromagnetic applications. For example, frequency selective surfaces [1] are used in radomes, EMC applications and dichroic subreflectors. Random rough surfaces, analyzed with respect to their scattering characteristics, are often treated as periodic structures constructed by repeating a suitable unit cell. Scattering from and analysis of array antennas also involve similar challenges and difficulties. Numerical algorithms based on integral equations have been used to study periodic structures for at least three decades. Zaki and Neureuther [2, 3] used the Method of Moments (MoM) [4] to analyze perfectly conducting surfaces with a profile of sinusoidal shape, where a unit cell of the periodic surface is treated by means of a Green's function for periodic arrays. Axline and Fung [5] employed the MoM to calculate the scattering from one dimensional random rough surfaces of metal. Nasir and Chew [6] studied periodic random rough surfaces using a MoM formulation based on Bloch's theorem to express the periodic fields and Green's functions. Petre et al. [7] employed a surface/volume integral equation formulation to analyze coated periodic strips. These methods can analyze a range of problems at any scan angle, but they are not particularly well-suited for scatterers with complex geometry. The finite element method (FEM) [8] is an attractive alternative because of its capabilities to model complex structures and inhomogeneous materials. Lou et al. [9] used FEM, in combination with a plane wave expansion for the scattered field, to calculate the scattering from two dimensional dielectric surfaces with a random rough profile.

Time-domain methods are advantageous in situations where a broad frequency band response of the structure is desired. Examples of popular time-domain methods are the finite-difference time-domain (FDTD) [10, 11] scheme and FEM in the time domain [8]. For normal incidence of a plane wave on a periodic structure, the boundary condition for a unit cell's periodic boundaries is rather easy to implement [12] since there is no time delay between such boundaries. Chan et al. [13] also used such a technique in their analysis of scattering from random rough surfaces at normal incidence by means of the FDTD scheme. For oblique angles of incidence, a time-domain formulation becomes more challenging with respect to the treatment of the periodic boundaries. There are some proposed solutions to this problem. One rather simple alternative [14, 15] is to use a time-harmonic source for a time-domain computation that is time stepped until a stationary state is reached. However, such an approach is monochromatic by nature and, thus, does not exploit the advantageous broad frequency band capabilities of time-domain simulations. Another technique is to transform Maxwell's equations so that the problems associated with time shift between the periodic boundaries can be avoided [16]. This procedure results in a new set of differential equations which can be discretized by techniques [17, 18, 19] that resemble the FDTD scheme. Unfortunately, conventional codes must often be modified before they can be used for such formulations and, moreover, the transformation typically implies a smaller Courant limit as compared to the original scheme [20]. Holter and Steyskal [21] developed yet another technique where a computational window is moved along the periodic structure and, thus, the difficulties associated with the time delay between the periodic boundaries of a unit cell can be avoided.

In this paper, we propose a new technique that is suitable for time-domain analysis of periodic structures excited by obliquely incident waves. It can easily be used with conventional implementations of time-domain schemes (e.g. the FDTD scheme or the time-domain FEM) without the need of substantial programming efforts, since it does not rely on transforming Maxwell's equations. Thus, the Courant condition and other stability properties of the underlying field solver are preserved. Our technique allows for an accurate analysis over a broad frequency band, which is accomplished by means of time-domain pulses with relatively short duration. The method is based on a carefully chosen incident wave such that it is feasible to use a trivial periodic boundary condition. This is accomplished by constructing the incident wave from a superposition of plane waves with an appropriate spatial variation along the periodic structure. Our technique can easily be generalized and used for three dimensional structures with an arbitrary polarized incident wave. In this paper, we present a derivation of the suggested method for transverse magnetic (TM) fields in two dimensions. The formulation for the corresponding transverse electric (TE) case is similar and can easily be derived in the same fashion. We present results for both the TM and TE polarization.

2 Formulation

Consider a two dimensional structure that is periodic in the x-direction, with the periodicity L as shown in figure 1. The periodic solution $\vec{E}(x + nL, y, t) = \vec{E}(x, y, t)$, where n is an integer, can easily be accounted for in most time-domain field solvers by means of simple relations between the fields on, and in the proximity of, the right and left boundaries. For such a situation, we construct an incident wave from a superposition of plane waves such that it satisfies this periodic requirement on the solution and, thus, the total field also exhibits the same periodic behavior.

An incident wave of the proposed type can be combined with different field solvers and, here, we use a stable hybrid [22] of the FEM and the FDTD scheme. The stable FEM-

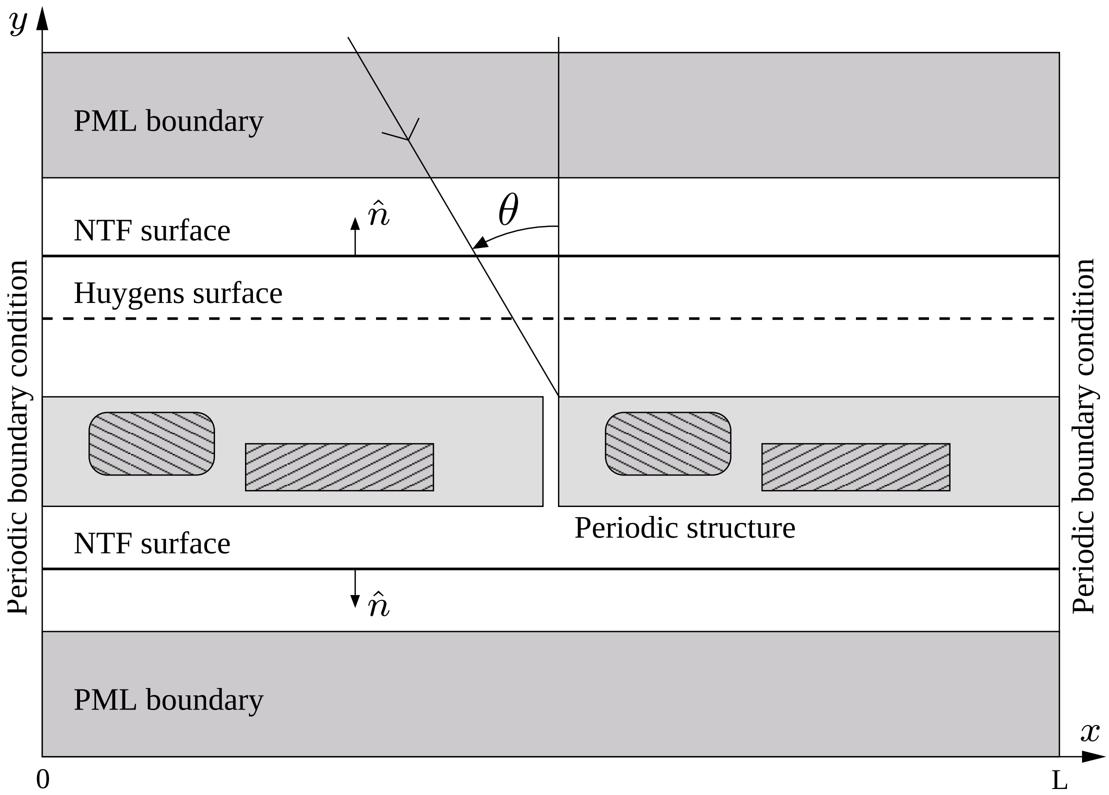

Figure 1: Geometry of a periodic structure.

FDTD hybrid allows for an unstructured FEM grid to discretize the periodic structure, which possibly involves complex geometry. The conventional FDTD is exploited in the homogeneous regions above and below the periodic structure. The incident wave is implemented by means of a so-called Huygen's surface [11], which is placed above the periodic structure. In order to calculate the amplitude of the reflected far field, we use a near-to-far (NTF) field transformation surface [11] above the Huygen's surface. Similarly, an NTF surface below the periodic structure is used to calculate the transmitted field in the far zone. The Huygen's surfaces and the NTF surfaces extend, along the periodic structure, across the entire computational region. The reflected and transmitted waves are absorbed by a perfectly matched layer (PML) [23, 24] placed along the top and bottom boundaries.

2.1 Quasi-planar incident wave

It is natural to use a single plane wave excitation for the computation of the scattering parameters since it fits well with the definition of the reflection and transmission coefficient. We construct a quasi-planar incident wave from a spectrum of plane waves with the amplitude $A(k_{\mathrm{y}})$ and a fixed wave number $k_{\mathrm{x}} = 2\pi n/L$ associated with the direction of periodicity, where the integer n can be used to control the angle of incidence. Consequently, the periodic boundary condition is also fulfilled by the reflected and transmitted field since their variation along the periodic structure is $k_{\mathrm{x}} + 2\pi m/L = 2\pi(n+m)/L$ for the m-th Floquet mode. The incident wave is then given by

$$E_{\mathrm{z,in}}(\vec{r},t) = \mathfrak{Re}\left\{\int_{-\infty}^{\infty} A(k_{\mathrm{y}}) e^{-jk_{\mathrm{x}}x - jk_{\mathrm{y}}y + jc(t-\tau)\sqrt{k_{\mathrm{x}}^2+k_{\mathrm{y}}^2}}\, dk_{\mathrm{y}}\right\} \tag{1}$$

where c is the speed of light and τ is a time delay. Some effects of the numerical dispersion errors, that are inherent in the FDTD scheme, may be reduced if the speed of light in (1) is replaced by the numerical phase velocity associated with an appropriately chosen center frequency of the incident spectrum of plane waves. The time-dependent near fields are transformed to the frequency domain by means of the discrete Fourier transform and, then, it is trivial to extract the information of interest such as the reflection and transmission coefficients of the periodic structure. It should be noted that this is feasible despite the variation in incident angles associated with a broad-band spectrum of plane waves.

A popular choice for time-domain excitations is a sinusoidal with a Gaussian amplitude modulation. Such a signal is optimal in the sense that the mean-square sense time-bandwidth product is the smallest possible [25]. In a similar manner, we choose the amplitude $A(k_{\mathrm{y}})$ as a Gaussian function multiplied with an additional exponential factor in order to (i) avoid plane waves that are close to grazing and (ii) achieve a relatively short time-domain pulse with rather well-localized frequency contents. For a wave that travels in the negative y-direction, the amplitude is given by

$$A(k_{\mathrm{y}}) = \begin{cases} E_0 \exp\left(-\left(\frac{k_{\mathrm{y}}-k_{\mathrm{y,c}}}{\kappa}\right)^2\right)\exp\left(-\alpha\frac{\kappa}{|k_{\mathrm{y}}|}\right), & k_{\mathrm{y}} \le 0 \\ 0, & k_{\mathrm{y}} > 0 \end{cases} \tag{2}$$

where $k_{\mathrm{y,c}}$ is the wave vector's y-component at the center frequency f_{c}, κ influences the frequency band width, α controls the near grazing contents and E_0 is the amplitude of the incident wave. If the factor $\exp(-\alpha\kappa/|k_{\mathrm{y}}|)$ is neglected, the choice $\kappa = \delta k_{\mathrm{y}}/\sqrt{2\ln(2)}$ gives a half-power bandwidth δk_{y} when expressed in terms of the wave vector's y-component, i.e. $A(k_{\mathrm{y,c}} \pm \delta k_{\mathrm{y}}/2) = E_0/\sqrt{2}$. A wave that travels in the positive y-direction is given by the expression (2) with $k_{\mathrm{y}} \le 0$ and $k_{\mathrm{y}} > 0$ exchanged.

Typically, the scattering properties of a periodic structure are sought at a center frequency f_{c} for a plane wave with some given incident angle. For the center frequency f_{c}, we may choose an appropriate combination of n and L such that $k_{\mathrm{x}} = 2\pi n/L = k_{\mathrm{c}}\sin\theta_{\mathrm{c}}$, where $k_{\mathrm{c}} = 2\pi f_{\mathrm{c}}/c$ and θ_{c} is sufficiently close to the desired incident angle. As a consequence, $k_{\mathrm{y,c}} = -k_{\mathrm{c}}\cos\theta_{\mathrm{c}}$ and, given these results, there are approximate expressions for the remaining parameters in (2) provided that θ_{c} is not too close to grazing and the bandwidth δf is sufficiently small in comparison to the center frequency f_{c}. Here, δf refers to the half-power bandwidth in terms of frequency, i.e. it is the frequency counterpart to δk_{y}. Below, we analogously use δk for the wavenumber and $\delta\theta$ for the angle of incidence. In such a situation, we use the approximate relation $\delta k_{\mathrm{y}} = \delta k/\cos\theta_{\mathrm{c}}$ to choose κ and $\alpha \ll |k_{\mathrm{y,c}}|/\kappa$, where $\delta k = 2\pi\delta f/c$. As a consequence, we get $\delta\theta \simeq (\delta k_{\mathrm{y}}/k_{\mathrm{c}})\sin\theta_{\mathrm{c}}$ where $k_{\mathrm{c}} = 2\pi f_{\mathrm{c}}/c$. This reasoning also shows that the angular spread $\delta\theta$ can be used to control the duration $\delta t \simeq 1/(2\delta f) \propto (\delta\theta)^{-1}$ of the the incident wave's time-domain pulse.

2.2 Scattering coefficient

The far field can be calculated by integrating the near-field, which is often referred to as a NTF field transformation [11]. The scattered field at a point $\vec{r} = r\hat{r}$ in the far field is given by

$$E_{\mathrm{z,sc}}(\vec{r},\omega) = \frac{e^{j\frac{3\pi}{4}}}{\sqrt{8\pi kr}} e^{-jkr} \int_C \left[\nabla E_{\mathrm{z}}(\vec{r}\,',\omega) - j\vec{k}^{\mathrm{sc}} E_{\mathrm{z}}(\vec{r}\,',\omega)\right] \cdot \hat{n}\ e^{j\vec{k}^{\mathrm{sc}}\cdot\vec{r}\,'}\,dl' \tag{3}$$

where $E_{\mathrm{z,sc}}$ is the scattered electric field, $\vec{k}^{\mathrm{sc}} = k\hat{r}$, $\hat{r} = \hat{x}\sin\vartheta + \hat{y}\cos\vartheta$ and ϑ is the scattering direction. (In the following, we denote the incident wave vector $\vec{k}^{\mathrm{in}} = k(\hat{x}\sin\theta - \hat{y}\cos\theta)$, which gives monostatic scattering for $\vartheta = -\theta$.) Figure 1 shows the NTF field transformation surface C and its normal $\hat{n}$. We introduce the scattering amplitude a_{z} as

$$a_{\mathrm{z}}(\vec{k}^{\mathrm{sc}}) = -\frac{1}{4}\int_C \left[\nabla E_{\mathrm{z}}(\vec{r}\,',\omega) - j\vec{k}^{\mathrm{sc}} E_{\mathrm{z}}(\vec{r}\,',\omega)\right] \cdot \hat{n}\ e^{j\vec{k}^{\mathrm{sc}}\cdot\vec{r}\,'}\,dl' \tag{4}$$

Due to the periodic solution, we only integrate over one unit cell from $x' = 0$ to $x' = L$. For a wave reflected into the upper half-space, the normal to the NTF surface is $\hat{n} = \hat{y}$ and the scattering amplitude can be written as

$$a_{\mathrm{z}}(\vec{k}^{\mathrm{sc}}) = -\frac{1}{4}\int_{x'=0}^{L} \left[\frac{\partial}{\partial y'} - jk_{\mathrm{y}}^{\mathrm{sc}}\right] E_{\mathrm{z}}(\vec{r}\,',\omega) e^{jk_{\mathrm{x}}x'}\,dx'\,e^{jk_{\mathrm{y}}^{\mathrm{sc}}y'} \tag{5}$$

Consider the simple case when the incident wave defined by (1) propagates through an empty unit cell (i.e. free space) and we calculate the scattered amplitude by means of the NTF transform (5). We insert the Fourier transform of (1) into (5) and arrive at

$$a_{\mathrm{z}}(\vec{k}^{\mathrm{sc}}) = -\frac{\pi}{4} e^{jk_{\mathrm{y}}^{\mathrm{sc}}y'} \int_{x'=0}^{L} -2jk_{\mathrm{y}}^{\mathrm{sc}} \frac{A(k_{\mathrm{y}}^{\mathrm{in}})}{v_{\mathrm{gy}}\left(k_{\mathrm{y}}^{\mathrm{sc}}\right)} e^{-jk_{\mathrm{y}}^{\mathrm{sc}}y'}\,dx'\,e^{-j\omega\tau} = j\frac{\pi}{2}k_{\mathrm{y}}^{\mathrm{sc}} L \frac{A(k_{\mathrm{y}}^{\mathrm{in}})}{v_{\mathrm{gy}}\left(k_{\mathrm{y}}^{\mathrm{sc}}\right)} e^{-j\omega\tau} \tag{6}$$

where $\vec{k}^{\mathrm{in}}$ and $\vec{k}^{\mathrm{sc}}$ are the wave-vectors of the incident and scattered fields respectively. Here, $v_{\mathrm{gy}}\left(k_{\mathrm{y}}^{\mathrm{sc}}\right) = c\cos\vartheta$ is the y-component of the group velocity for the scattered field. (Again, it is feasible to adjust v_{gy} with the objective of reducing dispersion errors.) Let us define the scattering coefficient Γ as the (complex) scattered field amplitude divided by the incident field amplitude. Then, the scattering coefficient must be unity for a wave traveling through free space which gives the scattering coefficient

$$\Gamma(\vec{k}^{\mathrm{in}},\vec{k}^{\mathrm{sc}}) = \frac{a_{\mathrm{z}}(\vec{k}^{\mathrm{sc}})}{A(k_{\mathrm{y}}^{\mathrm{in}})} \frac{v_{\mathrm{gy}}(k_{\mathrm{y}}^{\mathrm{sc}})}{j\frac{\pi}{2}k_{\mathrm{y}}^{\mathrm{sc}} L} e^{j\omega\tau}. \tag{7}$$

3 Numerical results

The proposed excitation technique for time-domain analysis of periodic structures is applied to three test cases: scattering from planar, sinusoidal and random rough surfaces.

These surfaces separate two dielectric half-spaces, where one is air and the other one is characterized by $\varepsilon_{\mathrm{r}} > 1$ and $\mu_{\mathrm{r}} = 1$. We exploit a stable FEM-FDTD hybrid [22] that uses an unstructured FEM grid in the vicinity of curved boundaries and a structured FDTD grid in the homogeneous space above and below the interface of the scattering surface. The maximum edge length in the FEM grid is smaller than or equal to the FDTD cell size denoted h. The time step is chosen according to the Courant limit of the FDTD [11], i.e. $\Delta t = h/(c_0\sqrt{2})$. We use a PML to absorb waves that propagate away from the scattering surface and it is backed by a perfect electric conductor (PEC). The PML has a monomial conductivity profile $\sigma(\xi) = \sigma_{\max}(\xi/w_{\mathrm{PML}})^m$ with $\sigma_{\max} = 0.8(m+1)/(Z_0 h)$ and $m = 3.5$, where w_{PML} is the thickness of the PML and ξ is the perpendicular distance to the interface between air and PML. The distance from the scattering surface to the PML is chosen such that the evanescent modes associated with the surface are sufficiently small given the thickness w_{PML} of the PML and its PEC backing.

3.1 Test 1 - Scattering from a planar dielectric half-space

The scattering of a plane wave from a planar interface at an oblique incident angle is analytically described by the Fresnel coefficients [26]. Consequently, this setting is appropriate for a convergence study and we use $\lambda_0/h = 8$, 16, 32 and 64 cells per wavelength, where λ_0 is the free-space wavelength at the center frequency $f_{\mathrm{c}} = 1$ GHz. We arbitrarily choose $L = 5\lambda_0$ and $n = 3$, which yields $\theta_{\mathrm{c}} \simeq 37°$. We let the region $y \leq 0$ be characterized by $\varepsilon_{\mathrm{r}} = 2.5$ and set the thickness of the PML to $w_{\mathrm{PML}} = \lambda_0$. Several values of $\delta\theta$ are also tested to verify that $\delta\theta$ has little or no influence on the convergence properties.

Figure 2 shows the error in the reflection coefficient as a function of the number of points per wavelength. We have second order convergence and the resolution $\lambda_0/h = 20$ gives a relative accuracy of roughly 1%, which is expected for a scheme based on linear elements. These results are basically independent of the angular widths $\delta\theta$ tested. The duration of the pulse with $\delta\theta = 10.00°$ is almost 10 times shorter than for $\delta\theta = 1.00°$ and, thus, the computation time can be reduced with almost the same factor.

3.2 Test 2 - Scattering from a sinusoidal surface

In the second test case, we consider scattering from a sinusoidal surface $s(x) = s_0 \sin(2\pi x/L)$, where the region $y \leq s(x)$ is a dielectric with $\varepsilon_{\mathrm{r}} = 5$ and $\mu_{\mathrm{r}} = 1$. The surface's height variation is $s_0 = 0.2\lambda_0$ and its period (and unit cell width) is $L = 5.2\lambda_0$, which gives 11 scattered plane waves that are reflected into the upper half plane.

The solid curve in figure 3 shows the monostatic scattering coefficient produced by a FEM-FDTD hybrid computation with the source proposed in this article. The hybrid uses $\lambda_0/h = 32$ cells per wavelength, a 32 cells thick PML and the angular spread of the incident wave is $\delta\theta = 5°$. Since analytical results are not easily available for this case, we used two other techniques to provide results for comparisons. Both these solvers use algorithms formulated in the frequency domain, where the treatment of the periodic structure and its excitation can be accounted for by well-established techniques. The dashed curve shows

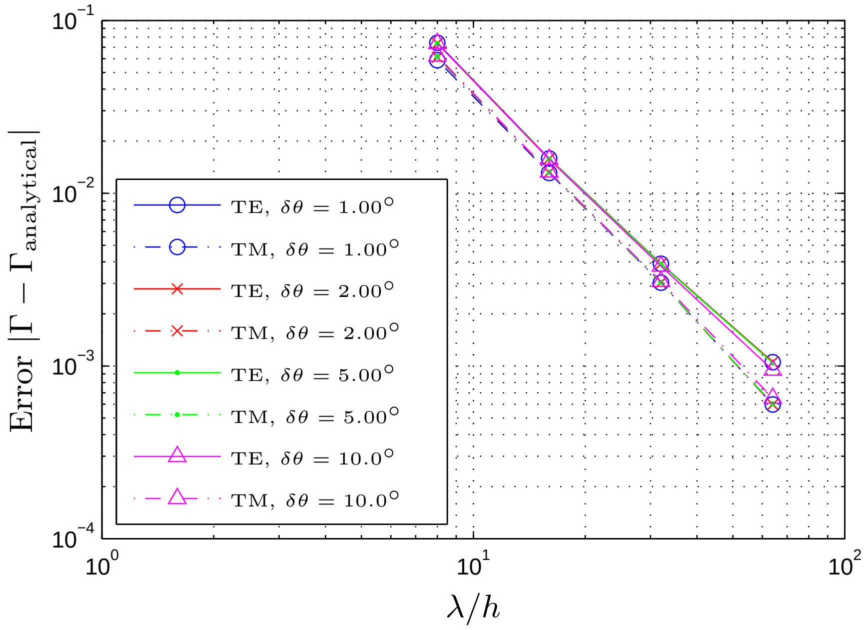

Figure 2: Error of the reflection coefficient as a function of the number of points per wavelength for a planar dielectric interface at an angle of incidence of $\theta_c = 37°$. The analytical reflection coefficients are $\Gamma_{\text{TE}} = -0.1551$ and $\Gamma_{\text{TM}} = -0.2929$ for the TE and TM cases respectively.

the results of an in-house field solver that expresses the solution in terms of Floquet modes along the x-direction and uses finite differences (FD) to discretize the resulting ordinary differential equations with respect to the y-direction. The electric field is expanded in 128 Floquet modes and, in the vertical direction, it is represented by a grid with $\lambda_0/h_{\text{FD}} = 128$ points per wavelength. The dash-dotted curve is computed by the commercial FEM based software `FEMLAB` [27] with a two wavelengths thick PML, fourth order elements and the cell size $h_{\text{FEMLAB}} = \lambda_0/10$.

The agreement is excellent between all methods for $|\theta| < 35°$. For angles of incidence larger than 35°, the monostatically scattered wave is very weak and the results are very sensitive to the resolution and other approximations that are a result of the discretization procedure adopted to solve the field problem.

3.3 Test 3 - Scattering from a random rough surface

Finally, we use the proposed method to calculate the scattering from a random rough surface with the Gaussian roughness spectrum $W(k) = (2\sqrt{\pi})^{-1} s_0^2 l \exp(-k^2 l^2/4)$ [28], where l is the correlation length and s_0 is the root-mean-square (RMS) height of the

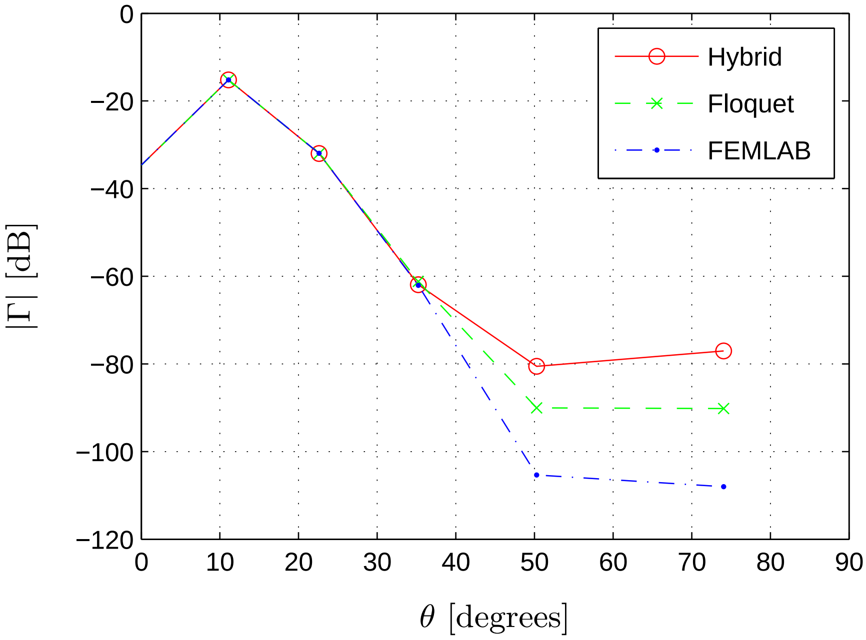

Figure 3: Scattering from a sinusoidal surface calculated using the novel method, a Floquet mode expansion technique and the commercial `FEMLAB` software.

surfaces. The rough surface is described by the curve

$$y = s(x) = \sqrt{\frac{2\pi}{L}} \sum_{n=-N}^{N} \xi_n \sqrt{W(k_n)} e^{jk_n x}, \tag{8}$$

where $k_n = 2\pi n/L$ and $\xi_n \in \mathcal{N}(0, 1/\sqrt{2}) + j\mathcal{N}(0, 1/\sqrt{2})$ such that $\xi_{-n} = \xi_n^*$. Here, the complex conjugate is denoted by the asterisk and $\mathcal{N}(m, \sigma)$ is the normal distribution with the expectation value m and the standard deviation σ. The dielectric half-space $y \leq s(x)$ below the rough surface is characterized by $\varepsilon_{\rm r} = 3.24$, which gives an index of refraction of 1.8.

For this last test case, we choose the correlation length $l = \lambda_0$, the RMS height $s_0 = 0.2\lambda_0$ and the periodicity $L = 30.2\lambda_0$, which is the same parameter combination studied by Lou et al. [9]. We use 50 surface realizations to calculate the mean scattering parameters. The angular spread of the incident wave is $\delta\theta = 5°$. The resolution of the FDTD grid is $h = \lambda_0/16$. Figure 4 shows the amplitude of the computed scattering coefficient Γ for monostatic and bistatic scattering with both TE and TM polarizations. The averaged value agree very well with the results obtained by Lou et al. [9].

4 Conclusions

We have developed a quasi-planar incident wave for time-domain scattering analysis of periodic structures, which is typically enforced on a Huygen's surface. Our technique

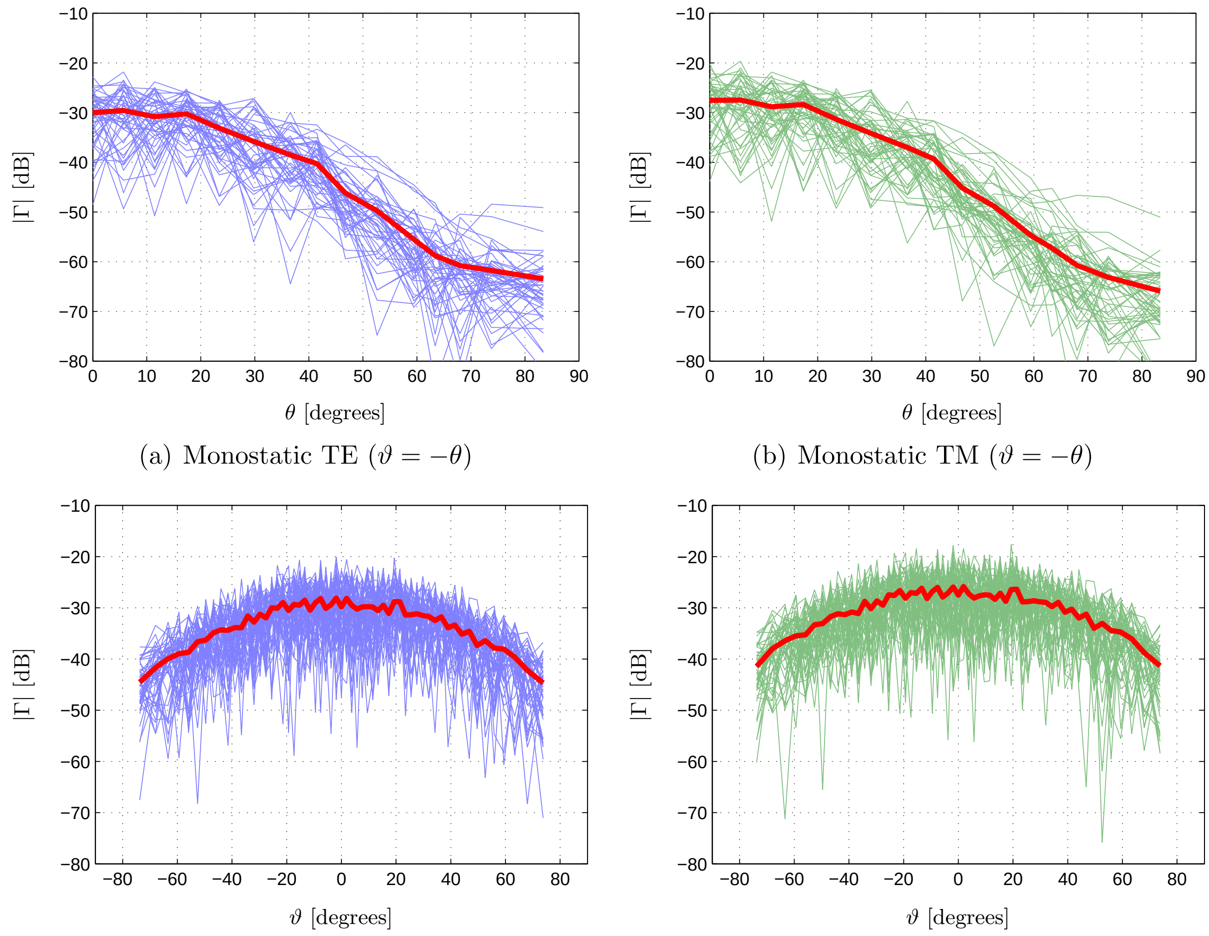

(a) Monostatic TE ($\vartheta = -\theta$)

(b) Monostatic TM ($\vartheta = -\theta$)

(c) Bistatic TE ($\theta = 0$)

(d) Bistatic TM ($\theta = 0$)

Figure 4: Computed bistatic and monostatic scattering coefficient Γ for both TE and TM polarization calculated for 50 surfaces.

constructs the incident wave from a superposition of plane waves with fixed propagation constant along the periodic structure. The duration of the incident wave can be controlled by means of its frequency spectrum or, equivalently, the angular spread in the plane waves. The method can rather easily be implemented in existing time-domain codes that support simple periodic boundary conditions and it does not influence the stability properties or the Courant condition of the time-domain field solver.

Tests demonstrate that a time-domain solver equipped with the proposed excitation converges as expected. For a stable FEM-FDTD hybrid method based on linear elements, second order convergence is achieved for smooth scatterers. A test with a planar interface between two different dielectrics shows that the error in the reflection coefficient is on the order of 1% when the resolution is $\lambda_0/h = 20$ points per wavelength. Similar results are achieved for surfaces with sinusoidal profile, where the reference solution is computed by means of frequency-domain field solvers based on a hybrid Floquet-FD solver and a higher order FEM.

Finally, we have used the method for scattering analysis of random rough surfaces, where the profile of the surface is generated by means of a Gaussian covariance function. The average of the reflection coefficient (based on 50 randomly selected surfaces) compares well with the corresponding results in the literature, where the two polarizations are considered separately for both monostatic and bistatic scattering. Computations based on our quasi-planar incident wave can be used for large problems and yield results with high accuracy. The possibility to use it for time-domain computations paves the way for efficient broad frequency band analysis of periodic structures.

References

[1] Ben A. Munk. *Frequency Selective Surfaces: Theory and Design*. Wiley-Interscience, New York, NY, April 2000.

[2] Kawthar A. Zaki and Andrew R. Neureuther. Scattering from a Perfectly Conducting Surface with a Sinusoidal Height Profile: TE Polarization. *IEEE Trans. Antennas Propag.*, AP-19(2):208–214, March 1971.

[3] Kawthar A. Zaki and Andrew R. Neureuther. Scattering from a Perfectly Conducting Surface with a Sinusoidal Height Profile: TM Polarization. *IEEE Trans. Antennas Propag.*, AP-19(6):747–751, November 1971.

[4] J. J. H. Wang. *Generalized Moment Methods in Electromagnetics*. John Wiley & Sons, New York, NY, 1991.

[5] R. M. Axline and Adrian K. Fung. Numerical Computation of Scattering from a Perfectly Conducting Random Surface. *IEEE Trans. Antennas Propag.*, AP-26(3):482–488, May 1978.

[6] Muhammad A. Nasir and Weng Cho Chew. Fast Solution of Scattering from Periodic Randomly Rough Infinite Surfaces. In *IEEE Antennas Propag. Soc. AP S Int. Symp.*, volume 3, pages 2020–2023. IEEE, June 1994.

[7] Peter Petre, Madhavan Swaminathan, Laszlo Zombory, Tapan K. Sarkar, and K. A. Jose. Volume/Surface Formulation for Analyzing Scattering from Coated Periodic Strips. *IEEE Trans. Antennas Propag.*, 42(1):119–122, January 1994.

[8] Jianming Jin. *The Finite Element Method in Electromagnetics*. John Wiley & Sons, New York, NY, 2nd edition, 2002.

[9] S. H. Lou, L. Tsang, and C. H. Chang. Application of the finite element method to Monte Carlo simulations of scattering of waves by random rough sufaces: penetrable case. *Waves Random Media*, 1(4):287–307, 1991.

[10] Kane S. Yee. Numerical solution of initial boundary value problems involving Maxell's equations in isotropic media. *IEEE Trans. Antennas Propag.*, 14(3):302–307, May 1966.

[11] Allen Taflove and Susan C. Hagness. *Computational Electrodynamics: the Finite-Difference Time Domain method*. Artech House, Inc, Norwood, MA, second edition, 2000.

[12] Wen-Jiunn Tsay and David M. Pozar. Application of the FDTD Technique to Periodic Problems in Scattering and Radiation. *IEEE Microw. Guid. Wave Lett*, 3(8):250–252, August 1993.

[13] C. H. Chan, S. H. Lou, L. Tsang, and J. A. Kong. Electromagnetic scattering of waves by random rough surface: a finite-difference time-domain approach. *Microw. Opt. Technol. Lett.*, 4(9):355–359, August 1991.

[14] Wei Lee Ko and Raj Mittra. Implementation of Floquet boundary condition in FDTD for FSS analysis. In *APS Int. Symp. Dig.*, volume 1, pages 14–17, 1993.

[15] Paul H. Harms, Raj Mittra, and Wai Ko. Implementation of the Periodic Boundary Condition in the Finite-Difference Time-Domain Algorithm for FSS Structures. *IEEE Trans. Antennas Propag.*, 42(9):1317–1324, September 1994.

[16] M. E. Veysoglu, R. T Shin, and J. A. Kong. A Finite-Difference Time-Dmain Analysis of Wave Scattering from Periodic Surfaces: Oblique Incidence Case. *J. Electromagn. Waves Appl.*, 7(12):1595–1607, 1993.

[17] Yin-Chun A. Kao and Robert G. Atkins. A Finite Difference-Time Domain Approach for Frequency Selective Surfaces at Oblique Incidence. In *IEEE Antennas Propag. Soc. AP S Int. Symp.*, volume 2, pages 1432–1435, July 1996.

[18] Amir Aminian and Yahya Rahmat-Samii. Spectral FDTD: A Novel Computational Technique for the Analysis of Periodic Structures. *IEEE Antennas Propag. Soc. AP S Int. Symp.*, 3:3139–3142, June 2004.

[19] J. Alan Roden, Stephen D. Gedney, Morris P. Kesler, James G. Maloney, and Paul H. Harms. Time-Domain Analysis of Periodic Structures at Oblique Incidence: Orthogonal and Nonorhogonal FDTD Implementations. *IEEE Trans. Microw. Theory Tech.*, 46(4):420–427, April 1998.

[20] Allen Taflove. *Advances in computational electrodynamics: the finite-difference time-domain method*. Artech House, Inc, Norwood, MA, 1998.

[21] Henrik Holter and Hans Steyskal. Infinite Phased Array Analysis Using FDTD Periodic Boundary Conditions — Pulse Scanning in Oblique Directions. *IEEE Trans. Antennas Propag.*, 47(10):1508–1514, October 1999.

[22] Thomas Rylander and Anders Bondeson. Stability of Explicit-Implicit Hybrid Time-Stepping Schemes for Maxwell's Equations. *J. Comput. Phys.*, 179(2):426–438, July 2002.

[23] Jean-Pierre Berenger. A Perfectly Matched Layer for the Absorption of Electromagnetic Waves. *J. Comput. Phys.*, 114(2):185–200, 1994.

[24] Zachary S. Sacks, David M. Kingsland, Robert Lee, and Jin-Fa Lee. A Perfectly Matched Anisotropic Absorber for Use as an Absorbing Boundary Condition. *IEEE Trans. Antennas Propag.*, 43(12):1460–1463, December 1995.

[25] Boualem Boashash. Estimating and Interpreting the Instantaneous Frequency of a Signal — Part 1: Fundamentals. *Proc. IEEE*, 80(4):520–538, 1992.

[26] Constatine A. Balanis. *Advanced Engineering Electromagnetics*. John Wiley & Sons, New York, NY, 1989.

[27] Comsol, `http://www.comsol.com/`. *Comsol*, March 2005.

[28] Leung Tsang, Jin Au Kong, and Kung-Hau Ding. *Scattering of Electromagnetic Waves*. Wiley, New York, 2001.

Chalmers Finite Element Center Preprints

2003–01 *A hybrid method for elastic waves*
Larisa Beilina

2003–02 *Application of the local nonobtuse tetrahedral refinement techniques near Fichera-like corners*
L. Beilina, S. Korotov and M. Křížek

2003–03 *Nitsche's method for coupling non-matching meshes in fluid-structure vibration problems*
Peter Hansbo and Joakim Hermansson

2003–04 *Crouzeix–Raviart and Raviart–Thomas elements for acoustic fluid–structure interaction*
Joakim Hermansson

2003–05 *Smoothing properties and approximation of time derivatives in multistep backward difference methods for linear parabolic equations*
Yubin Yan

2003–06 *Postprocessing the finite element method for semilinear parabolic problems*
Yubin Yan

2003–07 *The finite element method for a linear stochastic parabolic partial differential equation driven by additive noise*
Yubin Yan

2003–08 *A finite element method for a nonlinear stochastic parabolic equation*
Yubin Yan

2003–09 *A finite element method for the simulation of strong and weak discontinuities in elasticity*
Anita Hansbo and Peter Hansbo

2003–10 *Generalized Green's functions and the effective domain of influence*
Donald Estep, Michael Holst, and Mats G. Larson

2003–11 *Adaptive finite element/difference method for inverse elastic scattering waves*
Larisa Beilina

2003–12 *A Lagrange multiplier method for the finite element solution of elliptic domain decomposition problems using non-matching meshes*
Peter Hansbo, Carlo Lovadina, Ilaria Perugia, and Giancarlo Sangalli

2003–13 *A reduced P^1–discontinuous Galerkin method*
R. Becker, E. Burman, P. Hansbo, and M.G. Larson

2003–14 *Nitsche's method combined with space–time finite elements for ALE fluid–structure interaction problems*
Peter Hansbo, Joakim Hermansson, and Thomas Svedberg

2003–15 *Stabilized Crouzeix–Raviart element for the Darcy-Stokes problem*
Erik Burman and Peter Hansbo

2003–16 *Edge stabilization for the generalized Stokes problem: a continuous interior penalty method*
Erik Burman and Peter Hansbo

2003–17 *A conservative flux for the continuous Galerkin method based on discontinuous enrichment*
Mats G. Larson and A. Jonas Niklasson

2003–18 *CAD–to–CAE integration through automated model simplification and adaptive modelling*
K.Y. Lee, M.A. Price, C.G. Armstrong, M.G. Larson, and K. Samuelsson

2003–19 *Multi-adaptive time integration*
Anders Logg

2003–20 *Adaptive computational methods for parabolic problems*
Kenneth Eriksson, Claes Johnson, and Anders Logg

2003–21 *The FEniCS project*
T. Dupont, J. Hoffman, C. Johnson, R.C. Kirby, M.G. Larson, A. Logg, and R. Scott

2003–22 *Adaptive finite element methods for LES: Computation of the mean drag coefficient in a turbulent flow around a surface mounted cube using adaptive mesh refinement*
Johan Hoffman

2003–23 *Adaptive DNS/LES: a new agenda in CFD*
Johan Hoffman and Claes Johnson

2003–24 *Multiscale convergence and reiterated homogenization of parabolic problem*
Anders Holmbom, Nils Svanstedt, and Niklas Wellander

2003–25 *On the relationship between some weak compactnesses with different numbers of scales*
Anders Holmbom, Jeanette Silfver, Nils Svanstedt, and Niklas Wellander

2003–26 *A posteriori error estimation in computational inverse scattering*
Larisa Beilina and Claes Johnson

2004–01 *Computability and adaptivity in CFD*
Johan Hoffman och Claes Johnson

2004–02 *Interpolation estimates for piecewise smooth functions in one dimension*
Anders Logg

2004–03 *Estimates of derivatives and jumps across element boundaries for multi-adaptive Galerkin solutions of ODEs*
Anders Logg

2004–04 *Multi-adaptive Galerkin methods for ODEs III: Existence and stability*
Anders Logg

2004–05 *Multi-adaptive Galerkin methods for ODEs IV: A priori error estimates*
Anders Logg

2004–06 *A stabilized non-conforming finite element method for incompressible flow*
Erik Burman and Peter Hansbo

2004–07 *On the uniqueness of weak solutions of Navier-Stokes equations: Remarks on a Clay Institute prize problem*
Johan Hoffman and Claes Johnson

2004–08 *A new approach to computational turbulence modeling*
Johan Hoffman and Claes Johnson

2004–09 *A posteriori error analysis of the boundary penalty method*
Kenneth Eriksson, Mats G. Larson, and Axel Målqvist

2004–10 *A posteriori error analysis of stabilized finite element approximations of the helmholtz equation on unstructured grids*
Mats G. Larson and Axel Målqvist

2004–11 *Adaptive variational multiscale methods based on a posteriori error estimation*
Mats G. Larson and Axel Målqvist

2004–12 *Multi-adaptive Galerkin methods for ODEs V: Stiff problems*
Johan Jansson and Anders Logg

2004–13 *Algorithms for multi-adaptive time-stepping*
Johan Jansson and Anders Logg

2004–14 *Simulation of mechanical systems with individual time steps*
Johan Jansson and Anders Logg

2004–15 *Computational modeling of dynamical systems*
Johan Jansson, Claes Johnson, and Anders Logg

2004–16 *Adaptive variational multiscale methods based on a posteriori error estimation: Duality techniques for elliptic problems*
Mats G. Larson and Axel Målqvist

2004–17 *Ultraconvergence of an interpolated finite element method for some fourth-order elliptic problems*
Andrey B. Andreev and Milena R. Racheva

2004–18 *Adaptive variational multiscale methods based on a posteriori error estimation: energy norm estimates for elliptic problems*
Mats G. Larson and Axel Målqvist

2004–19 *Stabilized Lagrange multiplier methods for elastic contact with friction*
Per Heintz and Peter Hansbo

2005–01 *A posteriori error estimates for mixed finite element approximations of elliptic problems*
Mats G. Larson and Axel Målqvist

2005–02 *On the numerical modeling of quasi-static crack growth in linear elastic fracture mechanics*
Per Heintz

2005–03 *Irreversibility in reversible systems I: the compressible Euler equations in 1d*
Johan Hoffman and Claes Johnson

2005–04 *Irreversibility in reversible systems II: the incompressible Euler equations*
Johan Hoffman and Claes Johnson

2005–05 *A Compiler for Variational Forms*
Robert C. Kirby and Anders Logg

2005–06 *Topological optimization of the evaluation of finite element matrices*
Robert C. Kirby, Anders Logg, L. Ridgway Scott and Andy R. Terrel

2005–07 *Modeling of resistive wall mode and its control in experiments and ITER*
Yueqiang Liu, M.S. Chu, A.M. Garofalo, Y. Gribov, M. Gryaznevich, T.C. Hender, D.F. Howell, R.J. La Haye, M. Okabayashi, S.D. Pinches, H. Reimerdes, P. de Vries, and EFDA-JET contributors

2005–08 *Continuum gradient based shape optimization of conducting shields for power frequency magnetic field mitigation*
Yueqiang Liu, P. Sousa Jr., E. Salinas, P. Cruz and J. Daalder

2005–09 *A quasi-planar incident wave excitation for time-domain scattering analysis of periodic structures*
David Ericsson, Tomas Halleröd, Börje Emilsson, Anders Bondeson and Thomas Rylander

These preprints can be obtained from

`www.phi.chalmers.se/preprints`